ARTICLE IN PRESS

Available online at www.sciencedirect.com

ScienceDirect

Planetary and Space Science ▮ (▮▮▮▮) ▮▮▮–▮▮▮

Planetary and Space Science

www.elsevier.com/locate/pss

Dynamics of the Venus upper atmosphere: Outstanding problems and new constraints expected from Venus Express

S.W. Bougher[a,*], S. Rafkin[b], P. Drossart[c]

[a]*University of Michigan, Ann Arbor, MI, USA*
[b]*Southwest Research Institute, Boulder, CO, USA*
[c]*Observatoire de Paris, Meudon, France*

Accepted 10 April 2006

Abstract

A consistent picture of the dynamics of the Venus upper atmosphere from ~90 to 200 km has begun to emerge [e.g., Bougher, S.W., Alexander, M.J., Mayr, H.G., 1997. Upper Atmosphere Dynamics: Global Circulation and Gravity Waves. Venus II, CH. 2.4. University of Arizona Press, Tucson, pp. 259–292; Lellouch, E., Clancy, T., Crisp, D., Kliore, A., Titov, D., Bougher, S.W., 1997. Monitoring of Mesospheric Structure and Dynamics. Venus II, CH. 3.1. University of Arizona Press, Tucson, pp. 295–324]. The large-scale circulation of the Venus upper atmosphere (upper mesosphere and thermosphere) can be decomposed into two distinct flow patterns: (1) a relatively stable subsolar-to-antisolar (SS–AS) circulation cell driven by solar heating, and (2) a highly variable retrograde superrotating zonal (RSZ) flow. Wave-like perturbations have also been observed. However, the processes responsible for maintaining (and driving variations in) these SS–AS and RSZ winds are not well understood. Variations in winds are thought to result from gravity wave breaking and subsequent momentum and energy deposition in the upper atmosphere [Alexander, M.J., 1992. A mechanism for the Venus thermospheric superrotation. Geophys. Res. Lett. 19, 2207–2210; Zhang, S., Bougher, S.W., Alexander, M.J., 1996. The impact of gravity waves on the Venus thermosphere and O_2 IR nightglow. J. Geophys. Res. 101, 23195–23205]. However, existing data sets are limited in their spatial and temporal coverage, thereby restricting our understanding of these changing circulation patterns.

One of the major goals of the Venus Express (VEX) mission is focused upon increasing our understanding of the circulation and dynamical processes of the Venus atmosphere up to the exobase [Titov, D.V., Lellouch, E., Taylor, F.W., 2001. Venus Express: Response to ESA's call for ideas for the re-use of the Mars Express platform. Proposal to European Space Agency, 1–74]. Several VEX instruments are slated to obtain remote measurements (2006–2008) that will complement those obtained earlier by the Pioneer Venus Orbiter (PVO) between 1978 and 1992. These VEX measurements will provide a more comprehensive investigation of the Venus upper atmosphere (90–200 km) structure and dynamics over another period in the solar cycle and for variable lower atmosphere conditions. An expanded climatology of Venus upper atmosphere structure and wind components will be developed. In addition, gravity wave parameters above the cloud tops will be measured (or inferred), and used to constrain gravity wave breaking models. In this manner, the gravity wave breaking mechanism (thought to regulate highly variable RSZ winds) can be tested using Venus general circulation models (GCMs).

Keywords: Venus; Upper atmosphere; Dynamics

1. Introduction

A consistent picture of the large scale dynamics of the Venus upper atmosphere from ~90 to 200 km has emerged, in spite of the lack of in situ wind measurements (e.g., Bougher et al., 1997). This picture has been gleaned from an examination of Pioneer Venus Orbiter (PVO) neutral density (e.g. O, He, and H) and temperature distributions above ~130 km, PVO ultraviolet night airglow distributions, PVO dayglow emissions (e.g. atomic O), H-Lyman-α emissions, and limited ground-based observations of lower thermospheric winds. Visible and infrared O_2 nightglow distributions from Veneras 9 and 10, Galileo, PVO and the ground, and other minor species distributions (e.g. CO) have also been used to constrain upper mesospheric wind

*Corresponding author. Tel.: +1 734 6473585.
E-mail address: bougher@umich.edu (S.W. Bougher).

0032-0633/$ - see front matter © 2006 Elsevier Ltd. All rights reserved.
doi:10.1016/j.pss.2006.04.023

patterns (~90−110 km). Many of these data sets were reviewed by Bougher et al. (1997) and Lellouch et al. (1997). The global circulation of the Venus upper atmosphere is found to be much different from that of the Earth, and can be decomposed into two distinct flow patterns: (1) a stable subsolar-to-antisolar (SS–AS) circulation cell driven by solar (EUV-UV-IR) heating, and (2) a retrograde superrotating zonal (RSZ) flow that varies greatly over time.

Gravity waves are also believed to play a major role in Venus upper atmosphere dynamics. Wavelike density perturbations with horizontal scales of 100–600 km have been observed in the Venus thermosphere by the PVO Neutral Mass Spectrometer (Kasprzak et al., 1988, 1993). These perturbations have been shown to be consistent with vertically propagating gravity waves from a source region at/below ~80 km, well below thermospheric altitudes (Mayr et al., 1988). These thermospheric gravity waves may be launched from the Venus cloud region (50–70 km), propagate vertically, and break in the thermosphere, thereby providing a significant source of momentum and energy (e.g. Alexander, 1992). These same gravity waves may generate small scale vertical mixing (i.e. eddy diffusion) in the Venus upper atmosphere.

The processes responsible for maintaining (and driving variations in) these SS–AS and RSZ winds in the Venus upper atmosphere are still not well understood or quantified. For example, it is apparent from available spacecraft and ground-based observations that some type of deceleration mechanism is necessary to slow the pressure-driven upper atmosphere winds (e.g. Alexander, 1992; Zhang et al., 1996; Bougher et al., 1997). This is important since the net day-to-night upper atmosphere circulation results in downwelling and adiabatic heating on the nightside. This circulation must be regulated to maintain the observed cold nightside temperatures and the density structure. This deceleration is not symmetric in local time, because the net zonal winds appear stronger at the dusk versus the dawn terminator. The mechanism responsible for this deceleration and asymmetry is thought to be gravity wave breaking and subsequent momentum and energy deposition in the Venus thermosphere (Alexander, 1992; Zhang et al., 1996; Bougher et al., 1997). The large variability of the zonal winds between 90 and 110 km is also attributed to the changing nature of this wave breaking. However, only limited observations of gravity wave features are available to constrain the sources, their vertical propagation, and impacts at thermospheric heights (e.g Bougher et al., 1997).

An assortment of circulation models have been constructed to address the Venus upper atmosphere circulation (see review by Bougher et al., 1997). These multi-dimensional models serve both to reproduce the global wind tracers defined above (thereby constraining the circulation patterns), and also to investigate the underlying processes responsible for the maintenance and day-to-day variability of these circulation patterns. Gravity wave breaking has been implemented in some of these model simulations to slow pressure driven winds. However, it has been difficult for 3-D thermospheric circulation models to reproduce observed diurnal density, temperature, and airglow variations with a unique set of input parameters and wind fields (Bougher et al., 1997) (see Section 3.2).

In light of these outstanding uncertainties about the nature and dynamics of the Venus upper atmosphere, one of the major objectives of the Venus Express mission is to conduct a coherent study of the atmospheric temperature and wind structure at various levels of the Venusian atmosphere from the ground to ~200 km (Titov et al., 2001). The dynamical coupling of atmospheric regions can be addressed in a more comprehensive manner using such measurements. Specific VEX instruments (see Section 4) are designed to obtain remote measurements that will complement those obtained earlier by PVO between 1978 and 1992, thereby providing a more comprehensive investigation of the Venus upper atmosphere structure and dynamics over the solar cycle and for variable lower atmosphere conditions.

In this paper, we provide a brief review of currently available constraints for the circulation patterns of the Venus upper atmosphere. Outstanding problems related to our understanding of the physical processes regulating the changing wind components are then outlined. Finally, we describe how planned measurements by several VEX instruments will address these processes by providing a more comprehensive characterization of the Venus upper atmosphere circulation and its spatial and temporal variations. Global circulation models (GCMs) can then be exercised to interpret these data sets and elucidate the underlying physical processes.

2. Review of currently available constraints

The large day-to-night temperature (and corresponding pressure) gradients in the Venus thermosphere were expected to drive very strong (nearly 400 m/s) SS–AS winds (see reviews by Fox and Bougher, 1991; Bougher et al., 1997). However, an assortment of proxy indicators have been used to infer a global thermospheric circulation that is much weaker, and not purely symmetric about noon and midnight. Separate SS–AS and RSZ wind components have been gleaned from various density, temperature, and airglow measurements (NO, O_2, O, H) above ~90 km. However, no direct wind measurements exist to confirm thermospheric wind patterns, except for limited and low-resolution ground-based 4.7-μm observations over 100–145 km (Maillard et al., 1995). Upper mesospheric winds (85–110 km) have been measured directly from ground-based observations, inferred from latitudinal temperature gradients via the thermal wind equation, and estimated from density variations of CO. A proper sampling of these various proxy indicators (Sections 2.1–2.5) can be used to probe the winds of the Venus

upper atmosphere (upper mesosphere and thermosphere) from ~90 to 200 km. Table 1 of Lellouch et al. (1997) summarizes all available species, temperatures, and/or airglow emissions, their key sampling altitudes, and the corresponding implications for SS–AS and RSZ wind components in the Venus upper atmosphere. Diurnal variations in the eddy diffusion coefficient are also determined from O dayglow observations (see Section 2.4). Table 1 (of this paper) summarizes a subset of these existing wind proxies that will also be measured by new instruments onboard VEX (see Section 4).

2.1. Neutral species and temperature distributions (70–90 km, 130–200 km)

The most pronounced feature of the Venus thermosphere that suggests a strong subsolar-to-antisolar (SS–AS) wind system is the large contrast in temperatures and densities between day and night. Dayside to nightside exospheric temperatures are observed to drop from 300 to 100–110 K at solar maximum conditions. Therefore, the nightside upper atmosphere of Venus is more accurately characterized as a "cryosphere", since temperatures drop as a function of altitude from the mesopause (170 K) to the exobase (100–110 K) (see Fox and Bougher, 1991). This temperature difference between day and night gives rise to horizontal pressure gradients, which to first order should drive a strong SS–AS circulation cell in Venus's upper atmosphere (Dickinson and Ridley, 1977; Bougher et al., 1997). This single symmetric cell, driven by in situ solar (EUV-UV-IR) heating, likely exists. However, convergence of the nightside flow does not occur precisely at midnight as expected from a purely symmetric SS–AS wind pattern. The actual motions in Venus's thermosphere are likely a superposition of the SS–AS flow and a RSZ wind component. Light species distributions (i.e. hydrogen and helium densities) exhibit post-midnight maxima in accord with the westward superrotation of the upper atmosphere ($\geqslant$150 km), corresponding to RSZ wind speeds of the order of 50–100 m/s (see review by Bougher et al., 1997). In general, the weaker the RSZ wind component, the larger the day-to-night buildup in the light species densities, and the shorter is the time delay in the peak density after midnight. While this paradigm describing dynamical control of light species distributions in the Venus upper mesosphere and thermosphere has been generally demonstrated, other mechanisms may play a significant role in affecting these density distributions. For instance, spatially and temporally variable eddy diffusion may serve to modify O density distributions (see Section 2.4); exospheric transport may also regulate the lightest (e.g. H and He) species distributions (Bougher et al., 1997) (see Section 2.5).

Wind measurements and thermal winds inferred from latitudinal temperature gradients in the upper mesosphere (85–110 km) reveal significant temporal variability in zonal wind magnitudes (Lellouch et al., 1997). An overview of all direct wind measurements and inferences at mesosphere/thermosphere altitudes is given in Table 1 from Lellouch et al. (1997). Reversed latitudinal temperature gradients (warming from equator-to-pole) suggest zonal winds decrease in magnitude above the cloud tops (~65 km). However, on some occasions, modifications of the latitudinal gradients occur and maintain cyclostrophic balance (and strong zonal winds) up to ~105 km. Large day-to-day variations in zonal wind magnitudes are reflected in the O_2 visible and IR nightglow intensity distributions (see Section 2.2) (e.g. Crisp et al., 1996). A comprehensive climatology of such temperature and wind measurements is needed to characterize the Venusian upper mesosphere/lower thermosphere region. At this time, the mechanisms responsible for these large variations in equator-to-pole temperature gradients (and the resulting changes in the zonal wind magnitudes) are not well understood.

Table 1
Upper atmosphere wind proxies for the Venus Express era

Species/emissions/temperatures	Altitude range (km)	SS–AS winds (m/s)	RSZ winds (m/s)
Temperatures (IR and occultation)[a]	70–90		variable (weak)
O_2 IR (1.27-μm)[b]	95–110		highly variable (~10–50)
O_2 Visible (400–800 nm)[c]	100–130		weak ($\leqslant$30)
NO nightglow (UV)[d]	115–150	~200	40–60
O dayglow (130 nm)[e]	130–250		see Section 2.4
Temperatures (night)[f]	above 150	~200	~50–100
H dayglow (121.6-nm)[g]	above 150		~45–90
H and He densities[h]	above 150		~45–90

[a]References: Taylor et al. (1980), Schafer et al. (1990), Ross-Serote et al. (1995), Kliore (1985).
[b]Crisp et al. (1996), Bougher et al. (1997).
[c]Krasnopolsky (1983), Bougher and Borucki (1994).
[d]Stewart et al. (1980), Bougher et al. (1990), Gerard et al. (1981).
[e]Alexander et al. (1993).
[f]Niemann et al. (1980), Mayr et al. (1980), Mengel et al. (1989), Keating et al. (1980), Bougher et al. (1986, 1997).
[g]Paxton et al. (1985, 1988a,b).
[h]Niemann (1979), Brinton et al. (1980).

Ground based measurements of CO distributions can also be used to monitor the large scale circulation pattern between 90–110 km near the mesopause; i.e. CO densities are dynamically controlled in this altitude region (Lellouch et al., 1997). A nightside bulge in the CO distribution has been observed repeatedly, but its local time location is quite variable. These observations confirm the changing nature of the upper mesosphere, lower thermosphere RSZ winds and their variation with altitude. Systematic CO observations are difficult to obtain from ground-based observatories. Nevertheless, ongoing monitoring of CO density distributions is useful for constraining Venus upper mesosphere, lower thermosphere wind variations, in concert with O_2 visible and IR nightglow measurements (see Section 2.2).

2.2. O_2 visible and IR nightglow morphologies and intensities (95–130 km)

The O_2 airglow emissions in the near IR (1.27-μm) and visible (0.4−0.8 μm) wavelengths are formed from the radiative recombination of atomic O produced on the dayside (from CO_2 photolysis at 100–120 km) and transported to the nightside by the global circulation (Lellouch et al., 1997). These emissions are sensitive tracers of the net circulation over 95–110 km (1.27-μm) and ~100–130 km (visible) regions. Observed nightside integrated vertical intensities are highly variable from day-to-day (e.g. Crisp et al., 1996); enormous spatial and temporal variations have been seen in these emissions. These variations are likely caused by a number of factors, including: (1) large variations in the zonal wind speeds at these altitudes; (2) changing gravity wave breaking (momentum drag); and (3) Variable small scale mixing (eddy diffusion) on the Venus nightside (see Section 3.2). Three-dimensional GCM simulations (Bougher and Borucki, 1994) reproduce the gross features of these emissions, but not its detailed appearance. In particular, the available IR nightglow maps (e.g. Allen et al., 1992) show that the intensity distribution is generally not symmetric in latitude, often exhibits multiple local maxima, and shows striking variations on timescales as short as 1-h (Lellouch et al., 1997). Long-term monitoring of these O_2 nightglow features is required and latitude versus local time maps constructed (Lellouch et al., 1997) to (1) firmly establish the latitudinal distributions; (2) search for all scales of spatial and temporal variability; and (3) identify any correlations between local temperature anomalies and O_2 intensities (see Section 3.2).

2.3. Nitric oxide nightglow morphology and intensities (115–150 km)

The NO ultraviolet (UV) chemiluminescent nightglow is a sensitive tracer of the thermospheric circulation pattern over ~115–150 km. This nightglow is the result of N and O atoms being transported from their source on the dayside to the nightside where radiative recombination yields UV photons in the NO γ and δ bands (Feldman et al., 1979; Stewart and Barth, 1979; Stewart et al., 1980; Bougher et al., 1990). Planet-wide observations by the PVO ultraviolet spectrometer at solar maximum (Fig. 1) over 35 orbits were statistically averaged to show that the NO(0,1) δ-band nightglow typically exhibits a bright spot reaching 1.9 ± 0.6 kilo-Rayleigh (kR) near 0200 LT just south of the equator (Bougher et al., 1990; Stewart et al., 1980). The NO nightglow layer was found to exhibit a peak emission at 115 ± 2 km (Gerard et al., 1981). Solar minimum values of this nightglow intensity are predicted to be reduced by nearly a factor of three (Bougher et al., 1990), consistent with the reduced dayside sources (N and O atoms) and weaker thermospheric circulation during solar minimum conditions.

The horizontal brightness distribution of this NO airglow over the nightside reflects an approximate map of the downward flux of N-atoms being supplied from the Venus dayside. This nightside downward flux is regulated by the dayside net column N-production plus the strength of the day-to-night global circulation. NO nightglow maps can be used to monitor the changing strength of the separate SS–AS and RSZ wind components that comprise the net thermospheric wind system. In particular, the local time position of the average peak emission (“bright patch”) constrains the zonal thermospheric wind speeds in the ~115–150 km altitude region (Figs. 1 and 2) (Stewart et al., 1980; Bougher et al., 1990). On average, the 2-h offset of the average nightside peak emission toward the morning terminator implies RSZ winds in the lower thermosphere of roughly 40–60 m/s. These RSZ winds are superimposed upon SS–AS winds (symmetric about noon and midnight) of nearly 180–200 m/s. Clearly, individual orbit nightglow patches (Fig. 2) reveal a large spatial and temporal variability in the intensity distribution. Time scales of an Earth day or less are implied. This suggests a highly variable thermospheric circulation from day-to-day. Long-term monitoring of these NO nightglow features is needed to (1) confirm predicted solar cycle variations;

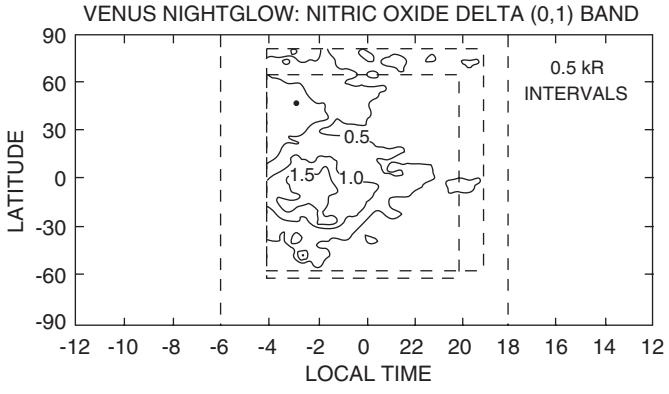

Fig. 1. The Pioneer Venus OUVS nitric oxide (0,1)δ-band vertical intensity distribution. A statistical map of 198.0 nm emission obtained over 35-orbits early in the PVO mission reveals a dark-disk average of 460 ± 120 R. Taken from Bougher et al. (1990).

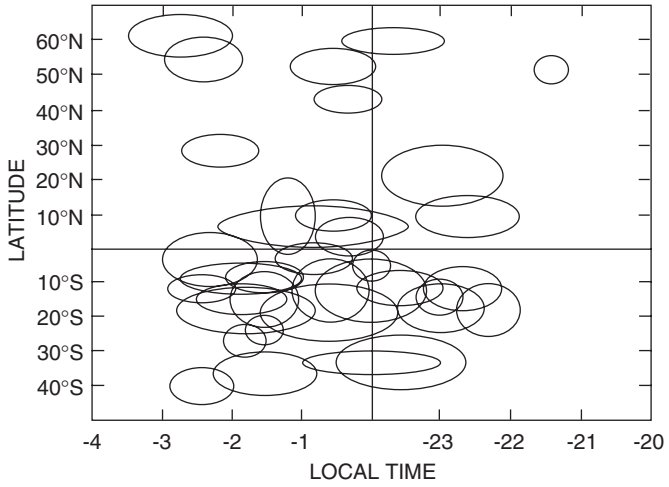

Fig. 2. The Pioneer Venus OUVS nitric oxide (0,1)δ-band vertical intensity distribution. Spatial variability of the observed nitric oxide individual bright airglow patches included in the statistical map of Fig. 1. The half-maximum intensity spatial extent of each individual NO patch is plotted as a function of local time and latitude. Taken from Bougher (1980).

(2) characterize the variability of the SS–AS and RSZ wind components in the 115–150 km altitude region; and (3) quantify the magnitude of gravity wave drag required to explain these observations.

2.4. *O dayglow and* O/CO_2 *mixing ratio morphologies (130–250 km)*

The atomic oxygen resonance transition between the $^3S^0$ and the ground state produces a triplet of bright (O~10 kR) emission lines near 130.4-nm (Bougher et al., 1997). The emission brightness is sensitive to the O/CO_2 ratio in the 130–250-km region in the thermosphere. O is the emitter and CO_2 efficiently absorbs the emission at altitudes below 125 km. Line center scattering optical depths near the excitation peak at 130 km are quite large, so the contribution function to the emergent intensity peaks much higher, near 155 km. The 130-nm brightness is rather insensitive to temperature changes, even those as large as 100 K. Alexander et al. (1993) analyzed a set of 130-nm images from the PVO Ultraviolet Spectrometer spanning 1980–1990. These images showed solar-locked emission patterns on the dayside (poleward of ~30° latitude), which are interpreted as global scale patterns in the O mixing ratio. These oxygen mixing ratios are up to a factor of 2.5 higher at the evening than the morning terminator, and cannot presently be explained by existing global thermospheric models. One explanation for this local time gradient is proposed in Alexander (1992), as a consequence of asymmetric turbulent mixing (eddy diffusion) due to breaking waves that originate at cloud levels. Monitoring of this dayglow emission (and its resulting dayside O-mixing ratio distributions) provides another constraint for the global thermospheric circulation and the underlying turbulent mixing variations.

2.5. *Lyman-alpha airglow morphology (above 150 km)*

The atomic-H distribution is a very sensitive tracer of the thermospheric circulation and the exospheric wind system above 150 km (see Fox and Bougher, 1991). The PVO Ultraviolet Spectrometer was able to make H-Lyman-α observations at regular intervals over the entire PVO mission, which spanned the solar cycle. The local time variation in the observed Lyman-α emission (Paxton et al., 1985, 1988a,b) seems consistent with the variation of atomic-H derived by Brinton et al. (1980); i.e. a strong H-bulge appears in the dawn sector just before the morning terminator. Furthermore, the H bulge also appears to increase in magnitude as solar activity decreases owing to a reduction in exospheric escape rates (see Donahue and Russell, 1997). In general, it is evident that H-atoms are being transported efficiently from the dayside to the nightside of the planet by the thermospheric wind system, with an asymmetry that is produced by superimposed RSZ winds above 150 km. In addition, an exospheric return flow, resulting from ballistic closed trajectories of H-atoms above the exobase, will modify the H-distribution from that otherwise produced solely by the thermospheric SS–AS and RSZ flow. Continued monitoring of this H distribution is needed to characterize the separate SS–AS, RSZ, and exospheric wind components at high altitudes.

3. Outstanding problems in upper atmosphere dynamics

3.1. *Variability of upper atmosphere wind components*

The processes responsible for maintaining and driving variations in the SS–AS and RSZ wind components in the Venus upper atmosphere are not well understood or quantified. In particular, what causes the rapid and spectacular variations observed in the magnitude of the RSZ flow, especially in the upper mesosphere and lower thermosphere regions (90–130 km)? Why is the structure of the NO (UV) and O_2 (visible and IR) nightglow emissions so complex and variable with time (e.g. diurnal and solar cycle timescales)? Why do hemispheric asymmetries in tracer emissions/species occur in the Venus upper atmosphere? Answers to these questions first require many more observations to establish a comprehensive climatology of the Venus atmospheric structure and wind components over ~90–200 km. A statistical assessment of the relative importance of the separate SS–AS and RSZ wind components during different atmospheric conditions can then be made.

The role of wave activity in potentially driving these large variations in Venus upper atmosphere wind components also remains to be addressed. Gravity wave breaking is one mechanism thought to be responsible for SS–AS wind deceleration and the asymmetries resulting in the observed RSZ flow in the upper atmosphere. Constraints for gravity wave parameters (i.e. cloud tops and above) are quite limited at present. Measurements of gravity wave

phase speeds and amplitudes (at various altitudes above the cloud tops) are crucial to the construction and validation of gravity wave breaking models. Confirmation of this mechanism will likely require the implementation of a self-consistent gravity wave breaking formulation into three-dimensional circulation models (Zhang et al., 1996; Bougher et al., 1997).

3.2. Current limitations and usage of global circulation models (GCMs)

Three-dimensional modeling tools are presently being used to study the Venus upper atmosphere circulation and the tracer emissions/species distributions (see reviews by Bougher et al., 1997, 2002). GCMs are crucial to synthesizing the various density, temperature, and airglow datasets for extracting winds. For instance, simulations have been conducted to reproduce the observations of the various airglow distributions (e.g. Bougher and Borucki, 1994; Bougher et al., 1990, 1997), thereby providing an estimate of the underlying SS–AS and RSZ wind components that vary over time. GCM tunable parameters include: (1) gravity wave parameters (Section 3.3); (2) eddy diffusion parameters (Section 2.4); (3) solar heating efficiencies and (4) CO_2 cooling rates (Keating and Bougher, 1992; Bougher et al., 1997). Solar fluxes are specified for the appropriate observation period being modeled.

Existing GCMs are presently unable to reproduce the observed diurnal density, temperature, and airglow variations utilizing a unique set of wind fields, eddy diffusion coefficients, and wave drag parameters (Bougher et al., 1997). This may reflect missing physical processes or inputs: (1) exospheric transport above 180–200 km; (2) planetary waves; and (3) limited gravity wave constraints for wave breaking. In general, too many free parameters presently exist. The modeling task would be greatly improved if: (1) simultaneous wind, temperature, and density measurements could be made over ~65–200 km; (2) gravity wave parameters could be quantified (Sections 3.1 and 3.3); and (3) circulation models could be extended to cover the region above the cloud tops to the exobase (~65–200 km). This extension permits a likely gravity wave source region (e.g. cloud tops), propagation region (above the cloud tops), and dissipation region (upper mesosphere and lower thermosphere) to be captured in the same three-dimensional model domain.

The small scale mixing arising from gravity wave processes can be parameterized in three-dimensional models using an eddy diffusion formulation. Limited modeling to date suggests that local variations in eddy diffusion parameters may play a significant role in controlling Venus nightglow intensity distributions and their rapid spatial and temporal variability (Bougher and Borucki, 1994; Bougher et al., 1997). Fig. 3 illustrates the response of three-dimensional model simulations to a 5-fold increase in the maximum eddy diffusion coefficient ($1.5 \times 10^7\ cm^2/s$). NO nightglow results from the radiative recombination of dayside produced N and O atoms as they descend on the nightside in response to the net thermospheric circulation. The altitude of the NO nightglow peak volume emission rate is determined to be a very sensitive indicator of the nightside eddy diffusion coefficient. Similarly, the local NO integrated vertical intensity varies as 3-body recombination and radiative recombination processes compete for importance within emitting layers at different altitudes (Stewart et al., 1980). A lower altitude for the O_2 emission layer (visible or IR) would also serve to smooth out horizontal intensity variations, since the timescales for dynamics and chemistry will be more nearly equal (Bougher and Borucki, 1994). New GCM simulations (including chemistry, eddy diffusion, and large scale winds), combined with VEX NO and O_2 nightglow intensity maps, and corresponding VEX vertical profiles of these emitting layers can be investigated together to address this variability.

Alternatively, Crisp et al. (1996) suggest that large daily variations in O_2 nightglow intensities may result from other local chemical or dynamical processes. The brightest airglow patches may be regions of strong subsidence (and local adiabatic warming) associated with strong downdrafts, where the O-atom supply and recombination rates are the largest. Conversely, dark areas might indicate regions of upwelling (and local adiabatic cooling). If this view is correct, spectral maps of the O_2 1.27-μm (IR) emission should show a positive correlation between the nightglow brightness and rotational (kinetic) temperature (Lellouch et al., 1997). Current data sets are not able to unambiguously confirm this relationship. New global

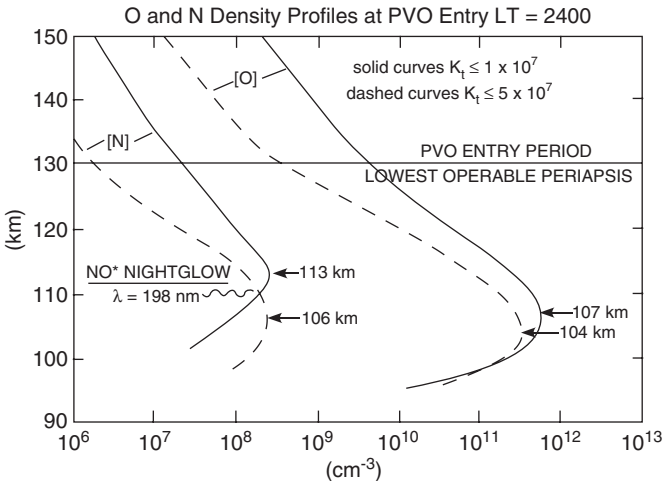

Fig. 3. Nightside density profiles of O and N atoms predicted for the period of PVO entry (2400 SLT) by the Venus Thermospheric General Circulation Model (VTGCM) code. Solar moderate conditions were assumed (F10.7 = 290 at Venus). Local nightside variations in eddy diffusion of a factor of 5 are predicted to have a large impact on the N and O density profiles and the corresponding nightglow layers (NO and O_2). A lower altitude for peak O_2 emission will serve to smooth out local time variations, since the timescales for dynamics and chemistry will be more nearly equal. Taken from Bougher and Borucki (1994).

model simulations and simultaneous VEX O_2 nightglow and temperature measurements can be assimilated to address this variability.

3.3. Uncertainties regarding gravity wave parameters and models

Simple gravity wave parameterizations, such as Rayleigh friction, cannot properly represent the true dynamical gravity waves processes in the Venus atmosphere. Whereas Rayleigh friction can only slow the mean circulation, gravity waves can either slow or accelerate the mean flow. Indeed, deposition of angular momentum has been invoked as a primary driver of lower atmosphere superrotation, something which cannot be achieved with Rayleigh friction. Gravity waves, putatively launched in the cloud top regions and propagating into the upper atmosphere, necessarily transport angular momentum corresponding to the strong zonal velocity ($\geqslant 100$ m/s) of the source region.

The gravity wave parameterizations of Lindzen (1981) and Holton (1982), based on the concept of gravity wave saturation can reproduce both acceleration and drag due to gravity waves by depositing energy and momentum between the breaking level and a critical level (should one exist). The breaking level is defined as the level at which the total atmospheric state (mean plus wave) results in an adiabatic lapse rate. Any additional perturbation above this level such as would be produced by a growing, vertically propagating wave, will result in a superadiabatic region subject to convective overturning (i.e, wave breaking). Still, the saturation region is a function of poorly constrained gravity wave properties and the mean state. However, gravity waves affect the mean state, and Venus GCM simulations indicate that gravity wave/mean flow interactions and feedback are not insignificant (Zhang et al., 1996).

Fritts and Lu (1993) have developed an advanced gravity wave parameterization for use in terrestrial GCMs based on the spectral characteristics of observed gravity waves on Earth. Such a scheme could be used for Venus, but requires knowledge of the gravity wave spectrum in the Venusian atmosphere (Zhang et al., 1996). Therefore, regardless of the parameterization, there remains substantial unknowns about the true nature of gravity waves in the atmosphere of Venus. Venus Express instrument measurements will help constrain these properties indirectly by quantifying the mean circulation more accurately than ever before (thereby constraining with greater fidelity the affects of gravity waves), and potentially directly through observations of wave perturbations of density, temperature, and atmospheric constituents.

4. Venus Express measurements providing wind constraints

The Venus Express mission is slated to conduct a coherent study of the atmospheric temperature and wind structure at various levels of the Venusian atmosphere from the ground to ~200 km (Titov et al., 2001). In particular, VEX remote measurements, will permit the first detailed study of the middle and upper atmosphere dynamics using O_2 (visible and IR nightglow), NO (UV nightglow), O (UV dayglow) and H (UV dayglow) emissions as tracers of the circulation. Details of the monitoring of these emissions by various VEX instruments, and their coordinated interpretation, will be addressed below. These constraints for the variable upper atmosphere circulation will be assimilated by various VEX teams to establish an extended climatology of the Venusian dynamics over ~90–200 km.

4.1. SPICAV UV and IR measurements

The Spectroscopy for Investigation of Characteristics of the Atmosphere of Venus (SPICAV) instrument is a versatile atmospheric spectrometer that consists of both UV (110–310 nm) and IR (0.7−1.7 μm) channels (Titov et al., 2001). SPICAV (UV) will be the first instrument at Venus to implement the solar/stellar occultation technique. SPICAV (IR) will systematically measure the nightside spectral emissions at high spectral resolution.

SPICAV (UV) is a sensitive (0.8 nm resolution) instrument with the intensified CCD detector operating in the photon-counting mode. Operational modes enable nadir, limb, and solar/stellar occultation measurements to be made. SPICAV (UV) will provide measurements of the vertical profiles of atmospheric density (and inferred temperatures) over 80–180 km (dayside) and 80–150 km (nightside) via stellar occultations. These day-to-night density and temperature variations can be used to validate global model (GCM) simulations and thereby extract Venus thermospheric SS–AS wind magnitudes (Section 3.2). Airglow (nadir and limb) observations of NO (190–270 nm), O (130.4 nm), H (121.6 nm), and CO (Cameron band) emissions will be made. Near apoapsis viewing of the nightside will provide global spectral imaging sequences of the NO nightglow, enabling maps to be constructed, from which estimates of the changing thermospheric RSZ wind component (~115–150 km) can be made. Periapsis limb viewing of the NO emission layer (highest vertical resolution) will provide further constraints on the changing nature of the local chemical and eddy diffusion processes on the nightside that regulate the nightglow intensity and its vertical distribution (Fig. 3).

Dayglow intensity distribution maps of O (130.4 nm) emissions can be analyzed, using a radiative transfer model, to unfold dayside O-mixing ratio distributions. Terminator differences in these mixing ratios reflect variations in eddy diffusion parameters, and the underlying gravity wave breaking processes (e.g. Alexander, 1992; Alexander et al., 1993). Lyman-α emissions are sensitive to day-to-night variations in H densities, from which estimates of the RSZ wind component at high thermospheric (or exospheric) altitudes can be made. Each of these UV proxy indicators yields information on the thermospheric

SS–AS and RSZ wind components over specific altitude regions (see Sections 2.3–2.5 and Table 1). Their combined information will help determine the dynamical processes that link the Venus middle and upper atmospheres (e.g. tides and planetary/gravity waves) through general circulation modeling of the upper atmosphere.

SPICAV (IR) is a miniature IR spectrometer (with 0.5–1.0 nm spectral resolution) based on acousto-optic tuneable filter (AOTF) technology. This instrument will be used to monitor the 1.27 μm emission with limb viewing. This high vertical resolution profile of the airglow layer, when combined with corresponding O_2 nightglow maps from VIRTIS, will provide a more comprehensive picture of the O_2 nightglow emitting layer (vertical distribution), and its spatial (horizontal) distribution. These inputs are crucial to constrain global model simulations that can be used to investigate the processes driving the temporal and spatial variability of this very intense emission (see Section 2.2).

4.2. VIRTIS visible and IR measurements

The Visible and Infrared Thermal Imaging Spectrometer (VIRTIS) instrument provides a low resolution spectral mapping (imaging) capability (VIRTIS-M channel 0.25−5.0 μm) that complements the high spectral resolution capability of the PFS instrument (see Section 4.3). VIRTIS also has a high spectral resolution channel, without imaging capabilities (VIRTIS-H) working in the 2−5 μm range, coaligned with VIRTIS-M. The description of the instrument and its observing goals is given in Drossart et al. (2006). VIRTIS observations will address upper atmosphere dynamics by: (1) measuring the 3-D temperature and derived thermal winds fields (60–90 km on the nightside); and (2) mapping the O_2 infrared and visible airglow as a tracer of the dynamics of the upper mesosphere and lower thermosphere (~95–130 km). The sequences of observations relevant to upper atmospheric dynamics correspond to Case 1 (near periapsis) and Case 2 (approaching apoapsis) observations (Titov et al., 2006), which focus upon local and global spectral imaging sequences of the disk of Venus, respectively.

Nightside VIRTIS spectral maps will be obtained at different times, with a typical spatial resolution between 0.5° and 3°. In particular, global maps will be obtained for the strong 1.27 μm O_2 emission, which was also observed from Galileo/NIMS (Drossart et al., 1993). Repeated observations during several orbits of Venus Express will allow us to monitor the IR airglow variability at different time scales between a few hours up to 10 days.

Thermal profiles retrieved from the 4.3 μm CO_2 band inversion (nightside), will be analyzed using the cyclostrophic equation to yield global wind fields, as demonstrated from Galileo/NIMS observations at Venus (Ross-Serote et al., 1995). By repeating such observations regularly, dynamical evolution of the wind pattern will be investigated.

Finally, the more speculative observation of non-LTE CO_2 emission in the 4.3 μm band (Roldan et al., 2000) should provide a sounding of the upper atmosphere (especially above 100 km). These emissions are expected to be easily observed from the limb, but also from the disk if they are strong enough. These 4.3 μm band emissions could be sensitive to atmospheric perturbations produced by gravity wave breaking; if observed, maps of the gravity wave perturbations could be obtained from the maps at these wavelengths.

4.3. PFS IR measurements

The Planetary Fourier Spectrometer (PFS) instrument provides high spectral resolution measurements spanning 0.9−45.0 μm. PFS global measurements of the temperature field (~55–100 km) will be used to determine the zonal component of the wind field (thermal wind) above the cloud tops. These inferred winds can be compared with similarly derived winds from the VIRTIS instrument (~60–90 km on the nightside). In addition, the $O_2(^1\Delta)$ airglow at 1.27 μm will be monitored (PFS limb observations), thereby characterizing the variations in the airglow layer over ~95–110 km (see Section 4.2 above). Complementary $O_2(^1\Delta)$ airglow maps generated by VIRTIS can be compared with these PFS limb measurements to investigate the changing intensity, plus horizontal and vertical distributions of this O_2 airglow emission. In this manner, the value of the O_2 airglow as a reliable tracer of the Venus circulation will be enhanced.

4.4. VeRa temperature and density measurements

The VeRA (Venus Radio Science) experiment will be used to derive vertical profiles of neutral mass density, temperatures, and pressure as a function of local time and season from the cloud deck (35–40 km) to ~100 km altitude. Temperature accuracy is expected to be approximately 0.1 K at the base and 10 K at the top of this sampling region. From these temperature measurements, the cyclostrophic equation can be applied to derive winds for comparison to independently inferred winds from the VIRTIS and PFS instruments (Sections 4.2 and 4.3).

4.5. VMC measurements

The Venus Monitoring Camera (VMC) has 4-separate objective lens systems, each of which images a different, filter selected wavelength range onto a quadrant of a common 1032 × 1024 pixel CCD detector. The VMC will utilize filters at 356 and 376-nm to image the O_2 visible nightglow (Section 2.2). VMC O_2 visible nightglow distribution maps can be coordinated and compared with corresponding VIRTIS O_2 IR nightglow maps in order to characterize the changing RSZ wind component for 2-overlapping airglow layers spanning ~95–130 km (see Table 1).

5. Summary and conclusions

Several Venus Express instruments (e.g. SPICAV, VIRTIS, PFS, VeRA, VMC) are scheduled to obtain remote measurements of various density, temperature, and airglow fields that will complement and extend the upper atmosphere record obtained earlier by the Pioneer Venus Orbiter and Galileo flyby. These new measurements will provide the basis for a more comprehensive (and coordinated) investigation of the Venus upper atmosphere structure and dynamics (90–200 km) over diurnal and solar cycle timescales, and for variable lower atmosphere conditions. These various data sets will be used to constrain general circulation models (GCMs), from which separate SS–AS and RSZ wind components can be extracted. A greatly expanded climatology of the Venus upper atmosphere structure and wind components will thus be compiled. In addition, gravity wave parameters above the cloud tops will be measured (or inferred), and used to constrain the gravity wave breaking model proposed by Alexander (1992); the feasibility of the gravity wave mechanism for regulating the SS–AS and RSZ wind components can be tested. Overall, our understanding of the underlying mechanism(s) responsible for maintaining and driving variations in the Venus upper atmosphere wind system will be significantly advanced.

Acknowledgments

We thank the Venus Express Project for supplying information needed regarding science objectives and instrument investigations planned. Both Bougher and Rafkin acknowledge NASA Venus Express Participating Scientist support.

References

Alexander, M.J., 1992. A mechanism for the Venus thermospheric superrotation. Geophys. Res. Lett. 19, 2207–2210.

Alexander, M.J., Stewart, A.I.F., Solomon, S.C., Bougher, S.W., 1993. Local time asymmetries in the Venus thermosphere. J. Geophys. Res. 98, 10849–10871.

Allen, D., Crisp, D., Meadows, V., 1992. Variable oxygen airglow on Venus as a probe of atmospheric dynamics. Nature 359, 516–518.

Bougher, S.W., 1980. The ultraviolet night airglow of Venus: morphology and implications. MS Thesis. University of Colorado, pp. 1–124.

Bougher, S.W., Borucki, W.J., 1994. Venus O_2 visible and IR nightglow: implications for lower thermosphere dynamics and chemistry. J. Geophys. Res. 99, 3759–3776.

Bougher, S.W., et al., 1986. Venus mesosphere and thermosphere: II. Global circulation, temperature and density variations. Icarus 68, 284–312.

Bougher, S.W., Gerard, J.C., Stewart, A.I.F., Fesen, C.G., 1990. The Venus nitric oxide night airglow: Calculations based on the Venus thermospheric general circulation model. J. Geophys. Res. 95, 6271–6284.

Bougher, S.W., Alexander, M.J., Mayr, H.G., 1997. Upper Atmosphere Dynamics: Global Circulation and Gravity Waves, Venus II, CH. 2.4. University of Arizona Press, Tucson, pp. 259–292.

Bougher, S.W., Roble, R.G., Fuller-Rowell, T.J., 2002. Simulations of the Upper Atmospheres of the Terrestrial Planets. In: Mendillo, M., Nagy, A., Waite, H. (Eds.), Comparative Aeronomy in the Solar System. AGU Monograph, pp. 261–288.

Brinton, H., et al., 1980. Venus nighttime hydrogen bulge. Geophys. Res. Lett. 7, 865–868.

Crisp, D., et al., 1996. Ground-based near-infrared observations of the Venus nightside: 1.27-μm $O_2(^1\Delta)$ airglow from the upper atmosphere. J. Geophys. Res. 101, 4577–4594.

Dickinson, R.E., Ridley, E.C., 1977. Venus mesosphere and thermosphere temperature structure: II. Day-night variations. Icarus 30, 163–178.

Donahue, T.M., Russell, C.T., 1997. The Venus atmosphere and ionosphere and their interaction with the solar wind: an overview. Venus II, CH. 1.1. University of Arizona Press, Tucson, pp. 3–31.

Drossart, P., Bzard, B., Encrenaz, T., Lellouch, E., Roos, M., Taylor, F.W., Collard, A.D., Calcutt, S.B., Pollack, J.B., Grinspoon, D., Carlson, R.W., Baines, K.H., Kamp, L.W., 1993. Search for spatial variations of the H_2O abundance in the lower atmosphere of Venus from NIMS-Galileo. Planet. Space Sci. 41, 495–504.

Drossart, P., et al., 2006. Scientific goals for the observation of Venus by VIRTIS on ESA/Venus Express mission. Planet. Space Sci. this issue.

Feldman, P.D., Moos, H.W., Clarke, J.T., Lane, A.L., 1979. Identification of the UV night airglow from Venus. Nature 279, 221.

Fox, J.L., Bougher, S.W., 1991. Structure, luminosity, and dynamics of the Venus thermosphere. Space Science Rev. 55, 357–489.

Fritts, D.C., Lu, W., 1993. Spectral estimates of gravity wave energy and momentum fluxes. Part II: parameterization of wave forcing and variability. J. Atmos. Sci. 50, 3695–3713.

Gerard, J.C., Stewart, A.I.F., Bougher, S.W., 1981. The altitude distribution of the Venus ultraviolet nightglow and implications on vertical transport. Geophys. Res. Lett. 8, 633–636.

Holton, J.R., 1982. The role of gravity wave induced drag and diffusion in the momentum budget of the mesosphere. J. Atmos. Sci. 39, 791–799.

Kasprzak, W.T., Hedin, A.E., Mayr, H.G., Niemann, H.B., 1988. Wavelike perturbations observed in the neutral thermosphere of Venus. J. Geophys. Res. 93, 11237–11246.

Kasprzak, W.T., Niemann, H.B., Hedin, A.E., Bougher, S.W., 1993. Wave-like perturbations observed at low altitudes by the Pioneer Venus Orbiter Neutral Mass Spectrometer during Orbiter entry. Geophys. Res. Lett. 20, 2755–2758.

Keating, G.M., Bougher, S.W., 1992. Isolation of major Venus thermospheric cooling mechanism and implications for Earth and Mars. J. Geophys. Res. 97, 4189–4197.

Keating, G.M., Nicholson, J.Y., Lake, L.R., 1980. Venus upper atmosphere structure. J. Geophys. Res. 85, 7941–7956.

Kliore, A.J., 1985. Recent results on the Venus atmosphere from Pioneer Venus radio-occultations. Adv. Space Res. 5, 41–49.

Krasnopolsky, V.A., 1983. Venus spectroscopy in the 3000-8000A region by Veneras 9 and 10. In: Hunten, D.M., Colin, L., Donahue, T.M., Moroz, V.I. (Eds.), Venus. University of Arizona Press, Tucson, pp. 681–765.

Lellouch, E., Clancy, T., Crisp, D., Kliore, A., Titov, D., Bougher, S.W., 1997. Monitoring of Mesospheric Structure and Dynamics. Venus II, CH. 3.1. University of Arizona Press, Tucson, pp. 295–324.

Lindzen, R.S., 1981. Turbulence and stress owing to gravity wave and tidal breakdown. J. Geophys. Res. 86, 9707–9714.

Maillard, J.-P., Lellouch, E., Crovisier, J., de Bergh, C., Bozard, B., 1995. Carbon monoxide 4.7 μm emission: a new dynamical probe of Venus' thermosphere. Bull. Amer. Astron. Soc. 27, 1080.

Mayr, H.G., et al., 1980. Dynamic properties of the thermosphere inferred from Pioneer Venus mass spectrometer measurements. J. Geophys. Res. 85, 7841–7847.

Mayr, H.G., Harris, I., Kasprzak, W.T., Dube, M., Varosi, F., 1988. Gravity waves in the upper atmosphere of Venus. J. Geophys. Res. 93, 11247–11262.

Mengel, J.G., Mayr, H.G., Harris, I., Stevens-Rayburn, D.R., 1989. Nonlinear three-dimensional spectral model of the Venusian thermosphere with superrotation: II. Temperature, composition, and winds. Planet. Space Sci. 37 (6), 707–722.

Niemann, H.B., 1979. Venus upper atmosphere neutral gas composition: First observations of the diurnal variations. Science 205, 54–56.

Niemann, H.B., et al., 1980. Mass spectrometer measurements of the neutral gas composition of the thermosphere and exosphere of Venus. J. Geophys. Res. 85, 7817–7827.

Paxton, L.J., Anderson, D.E., Stewart, A.I.F., 1985. The Pioneer Venus Orbiter Ultraviolet Spectrometer experiment: analysis of H-Lyman-α data. Adv. Space Res. 5 (9), 129–132.

Paxton, L.J., Anderson, D.E., Stewart, A.I.F., 1988a. Analysis of the Pioneer Venus ultraviolet spectrometer Lyman-α data from near the subsolar region. J. Geophys. Res. 93, 1766–1772.

Paxton, L.J., Anderson, D.E., Stewart, A.I.F., 1988b. Correction to: analysis of the Pioneer Venus ultraviolet spectrometer Lyman-α data from near the subsolar region. J. Geophys. Res. 93, 11551.

Roldan, C., Lopez-Valverde, M.A., Lopez-Puertas, M., Edwards, D.P., 2000. Non-LTE infrared emissions of CO_2 in the atmosphere of Venus. Icarus 147, 11.

Ross-Serote, M., Drossart, P., Encrenaz, Th., Lellouch, E., Carlson, R.W., Baines, K.H., Taylor, F.W., Calcutt, S.B., 1995. The thermal structure and dynamics of the atmosphere of Venus between 70 and 90 km from Galileo-NIMS spectra. Icarus 114, 300–309.

Schafer, K., et al., 1990. Infrared Fourier-spectrometer experiment from Venera-15. Adv. Space Res. 10 (5), 57–66.

Stewart, A.I., Barth, C.A., 1979. Ultraviolet night airglow of Venus. Science 205, 59.

Stewart, A.I.F., Gerard, J.C., Rusch, D.W., Bougher, S.W., 1980. Morphology of the Venus ultraviolet night airglow. J. Geophys. Res. 85, 7861–7870.

Taylor, F.W., et al., 1980. Structure and meteorology of the middle atmosphere of Venus: infrared remote sensing from the Pioneer Orbiter. J. Geophys. Res. 85, 7963–8006.

Titov, D.V., Lellouch, E., Taylor, F.W., 2001. Venus Express: Response to ESA's call for ideas for the re-use of the Mars Express platform. Proposal to European Space Agency, 1–74.

Titov, D.V., et al., 2006. Venus Express Science planning. Planet. Space Sci. this issue, doi:10.1016/j.pss.2006.04.017.

Zhang, S., Bougher, S.W., Alexander, M.J., 1996. The impact of gravity waves on the Venus thermosphere and O_2 IR nightglow. J. Geophys. Res. 101, 23195–23205.